nature immunology

The T helper type 2 response to cysteine proteases requires dendritic cell–basophil cooperation via ROS-mediated signaling

Hua Tang[1], Weiping Cao[1], Sudhir Pai Kasturi[1], Rajesh Ravindran[1], Helder I Nakaya[1], Kousik Kundu[2], Niren Murthy[2], Thomas B Kepler[3], Bernard Malissen[4] & Bali Pulendran[1,5]

The mechanisms that initiate T helper type 2 (T_H2) responses are poorly understood. Here we demonstrate that cysteine protease–induced T_H2 responses occur via 'cooperation' between migratory dermal dendritic cells (DCs) and basophils positive for interleukin 4 (IL-4). Subcutaneous immunization with papain plus antigen induced reactive oxygen species (ROS) in lymph node DCs and in dermal DCs and epithelial cells of the skin. ROS orchestrated T_H2 responses by inducing oxidized lipids that triggered the induction of thymic stromal lymphopoietin (TSLP) by epithelial cells mediated by Toll-like receptor 4 (TLR4) and the adaptor protein TRIF; by suppressing production of the T_H1-inducing molecules IL-12 and CD70 in lymph node DCs; and by inducing the DC-derived chemokine CCL7, which mediated recruitment of IL-4$^+$ basophils to the lymph node. Thus, the T_H2 response to cysteine proteases requires DC-basophil cooperation via ROS-mediated signaling.

Immune responses to T cell–dependent antigens show striking heterogeneity in terms of the cytokines made by helper T cells and the class of antibody secreted by B cells. In response to intracellular microbes, CD4$^+$ helper T cells differentiate into T helper type 1 (T_H1) cells, which produce interferon-γ (IFN-γ); in contrast, helminths induce the differentiation of T_H2 cells, whose cytokines (principally interleukin 4 (IL-4), IL-5 and IL-13) induce immunoglobulin E (IgE) and eosinophil-mediated destruction of the pathogens[1,2]. Furthermore, T_H17 cells (IL-17-producing helper T cells) mediate protection against fungal infections[3]. In addition to those subsets, other subsets have been identified, including T_H9 cells (IL-9-producing helper T cells), T_H22 cells (IL-22-producing helper T cells) and follicular helper T cells, located in the B cell–rich follicles of lymphoid organs[2]; but their physiological relevance and relationship to T_H1, T_H2 and T_H17 cells are still being defined. Although much is known about the cytokines produced early in the response and the transcription factors that determine helper T cell polarization, the early 'decision-making' mechanisms that result in a given helper T cell response remain poorly understood. There is now ample evidence of a fundamental role for dendritic cells (DCs) in this process[4–6]. DCs comprise several functionally distinct subsets, which express a wide array of pathogen-recognition receptors (PRRs), including Toll-like receptors (TLRs); these enable them to 'sense' microbes[7].

Despite the increasing knowledge about how the innate immune system shapes T_H1 and T_H17 responses, very little is known about its effect on T_H2 responses. Basophils and mast cells promote T_H2 responses by rapidly producing IL-4 after crosslinking of their Fc receptor for IgE (FcεRI) through preexisting antigen-IgE complexes[8–13]. Basophils can also prime T_H2 responses to helminths and protein allergens[14–16]. Despite such advances, the potential importance of DC subsets and PRRs in sensing helminths or protein allergens and in 'programming' T_H2 immunity remains largely unknown.

Although certain TLR ligands and ligands for the cytosolic PRR Nod1 induce T_H2 responses[17–21], the extent to which such receptors are involved in the initiation of T_H2 responses to classic T_H2 stimuli such as protease allergens or helminths is unknown. Furthermore, there is now a substantial body of data on the vital importance of DCs in modulating T_H2 responses. Distinct subsets of DCs induce T_H2 responses differently[22,23], and specific microbial stimuli and allergens can 'program' DCs to prime T_H2 responses[24]. Consistent with those findings, depletion of DCs abrogates asthma in mice[25]. Despite evidence of the involvement of DCs in T_H2 responses, very little is understood about the nature of the DC subsets that induce T_H2 responses *in vivo*, how DCs sense T_H2-inducing stimuli, the nature of the intracellular signaling pathways that 'program' DCs to induce T_H2 responses, and whether DCs act in concert with other cell types such as mast cells and basophils (which produce copious IL-4) to orchestrate T_H2 responses. In addition, the role of DCs in initiating T_H2 responses has been challenged by a published study suggesting that DCs are neither necessary nor sufficient for a T_H2 response induced by papain[15].

[1]Emory Vaccine Center, Atlanta, Georgia, USA. [2]Department of Biomedical Engineering, Georgia Institute of Technology, Atlanta, Georgia, USA. [3]Center for Computational Immunology, Duke University, Durham, North Carolina, USA. [4]Centre d'Immunologie de Marseille-Luminy, Institut National de la Santé et de la Recherche Médicale U631, Centre National de la Recherche Scientifique Unité Mixte de Recherche 6102, Université de la Méditerranée, Marseille, France. [5]Department of Pathology, Emory University, Atlanta, Georgia, USA. Correspondence should be addressed to B.P. (bpulend@emory.edu).

Received 4 January; accepted 3 May; published online 23 May 2010; doi:10.1038/ni.1883

Here we demonstrate that migratory skin-derived dermal DCs were essential to the induction of a T_H2 response to the cysteine protease papain. Subcutaneous immunization with papain plus antigen induced reactive oxygen species (ROS) in lymph node DCs and in dermal DCs and epithelial cells of the skin. ROS orchestrated T_H2 responses by inducing oxidized lipids that triggered induction of thymic stromal lymphopoietin (TSLP) mediated by TLR4 and the adaptor TRIF in epithelial cells, by suppressing production of the T_H1-inducing molecules IL-12 and CD70 by lymph node DCs, and by inducing the DC-derived chemokine CCL7, which mediated the recruitment of IL-4$^+$ basophils to the lymph node.

RESULTS

DCs and T_H2 differentiation *in vivo*

The cysteine protease papain, when injected together with ovalbumin protein (OVA), induced OVA-specific IgE and IgG1 antibodies and IL-4-producing CD4$^+$ T cells (**Fig. 1a**), as described before[15,26]. In contrast, CpG DNA plus OVA stimulated IFN-γ-producing CD4$^+$ T cells and OVA-specific IgG2b antibodies (**Fig. 1a**). Bromelain, a related cysteine protease, also induced T_H2 responses (**Supplementary Fig. 1**). To determine whether DCs were required for induction of the T_H2 response to OVA plus papain, we used the transgenic CD11c–diphtheria toxin receptor (CD11c-DTR) mouse model[27]. We selectively and transiently depleted CD11c-DTR mice of DCs by systemic administration of diphtheria toxin before immunizing the mice with OVA plus papain. Analysis by flow cytometry showed that intraperitoneal injection of diphtheria toxin into CD11c-DTR mice resulted in efficient depletion of DCs from lymph nodes and the dermis (**Supplementary Fig. 2**). We immunized CD11c-DTR and wild-type mice with OVA plus papain 24 h after injection of diphtheria toxin. After immunization, the production of IL-4 by CD4$^+$ T cells was much lower in mice depleted of DCs (**Fig. 1b**). These results demonstrate that DCs are required for the induction of a T_H2 response to papain. To further confirm the role of DCs in inducing antigen-specific T_H2 responses, we transferred various numbers of CD4$^+$ OT-II (ovalbumin-specific T cell antigen receptor) T cells into wild-type mice or CD11c-DTR mice (depleted of DCs by injection of diphtheria toxin) and then immunized the mice with OVA plus papain. We collected draining lymph node cells 4 d after immunization and restimulated the cells for 4 d *ex vivo* with OVA peptide (amino acids 323–339). After depletion of DCs, IL-4 production by CD4$^+$ T cells was much lower (**Fig. 1c**). Together, these data demonstrate that DCs are required for the induction of antigen-specific T_H2 responses in response to papain.

Peripheral tissue–resident DCs take up antigen and migrate to draining lymph nodes to initiate adaptive immune responses[4–6]. Given that stimulation with papain effectively induced DC migration to and accumulation in the draining lymph node[15,26], we hypothesized that skin-derived DCs have a critical role in the induction of T_H2 responses to papain. To determine the role of skin-derived DCs, we blocked the migration of skin DCs in mice by injecting pertussis toxin or Bw245c (an agonist of the prostanoid receptor DP1), each of which can inhibit the migration of skin DCs[28]. To monitor T_H2 responses *in vivo*, we used 4get mice, in which IL-4 production can be detected by flow cytometry analysis of the expression of green fluorescent protein[29]. We treated 4get mice with pertussis toxin or Bw245c before immunizing them with OVA plus papain and examined IL-4 secretion by CD4$^+$ T cells in the draining lymph nodes. Treatment with either pertussis toxin or Bw245c resulted in much less IL-4 production by CD4$^+$ T cells (**Fig. 1d**). This experiment suggested that the papain-induced T_H2 response was dependent on the migration of skin-derived DCs to the draining lymph nodes. To further confirm that finding, we immunized 4get mice in the ear with OVA plus papain and then excised the injection site 6 h after immunization to physically block the migration of skin DCs[28,30]. IL-4 production by CD4$^+$T cells from mice that underwent excision of the injection site was much lower than that of cells from mice with an intact site of immunization (**Fig. 1e**). To exclude the possibility that excision of the injection site could result in removal of the antigen depot, thus potentially diminishing presentation by any cell type, we determined whether we could visualize OVA or papain in the draining lymph node before excision of the site. Consistent with published reports[30], at 2 h after immunization with labeled OVA or labeled papain, we detected a large amount of fluorescence in the subcapsular sinus and the underlying area between the B cell–rich follicles (**Fig. 1f** and **Supplementary Fig. 3**). Consistent with published studies[30], it is very likely that soluble protein reached the lymph node via the lymphatic vessels. Therefore, excision of the injection site at 6 h does not preclude antigen availability in the lymph node. Together, these data (**Fig. 1d–f**) suggest that the skin-derived migratory DCs have a prominent role in the induction of T_H2 responses after stimulation with papain.

The skin is populated by at least two subsets of DCs: epidermal Langerhans cells and resident dermal DCs. To investigate which skin DC subset was involved in the T_H2 response to papain, we used a transgenic langerin-DTR mouse model in which Langerhans cells could be completely ablated within 24 h of the injection of diphtheria toxin[31] and the epidermis remained largely devoid of Langerhans cells for at least 4 weeks after injection of diphtheria toxin (**Supplementary Fig. 4**). We immunized mice at day 14 after treatment with diphtheria toxin, a time at which other langerin-positive cells in the dermis would have returned[31,32]. There was no noticeable change in the induction of the T_H2-dependent OVA-specific IgG1 antibody response after depletion of Langerhans cells (**Fig. 1g**). In fact, we observed significantly more IL-4 production by CD4$^+$ T cells isolated from langerin-DTR mice treated with diphtheria toxin than by cells from wild-type mice (**Fig. 1g**). These data demonstrate that papain-induced T_H2 responses were not promoted by Langerhans cells. We therefore sought to determine if the T_H2 response was dependent on dermal DCs. We immunized C57BL/6 mice with Alexa Fluor 488–labeled papain or Alexa Fluor 647–labeled OVA plus papain, then analyzed the uptake of labeled papain or labeled OVA and their distribution in various DC subsets in the draining lymph node at 24 h after immunization (**Fig. 1h,i**). First, we identified CD11c$^+$B220$^-$ 'conventional' DCs, then we used the expression of CD8α and the DC marker DEC-205 on this subset to resolve four main DC subsets in the lymph node as described before[33]. Here CD8α$^+$DEC-205$^+$ cells are CD8α$^+$ DCs, CD8α$^-$DEC-205^{hi} cells are Langerhans cells, CD8α$^-$DEC-205$^+$ cells are dermal DCs, and CD8α$^-$DEC-205$^-$ cells are CD8α$^-$ DCs[33]. We found that dermal DCs were the main population of cells that contained both papain and OVA. In contrast, immunization with OVA plus lipopolysaccharide (LPS) resulted in the 'preferential' uptake of antigen by CD8α$^+$ DCs (**Fig. 1h,i**). A subset of DCs in the dermis has been shown to express CD103 (refs. 32,34,35). To determine if that subset was involved in antigen uptake, we stained draining lymph node cells from mice immunized with labeled papain and OVA by using a panel of flow cytometry antibodies as described[36] (**Supplementary Fig. 5**) and did not find CD103$^+$ DCs that efficiently took up antigen (**Supplementary Fig. 6**).

To further investigate the ability of each DC subset to present antigen to T cells, we sorted the four main conventional DC subsets by flow cytometry from the draining lymph node after immunization with OVA, OVA plus papain, or OVA plus LPS, and then cultured those

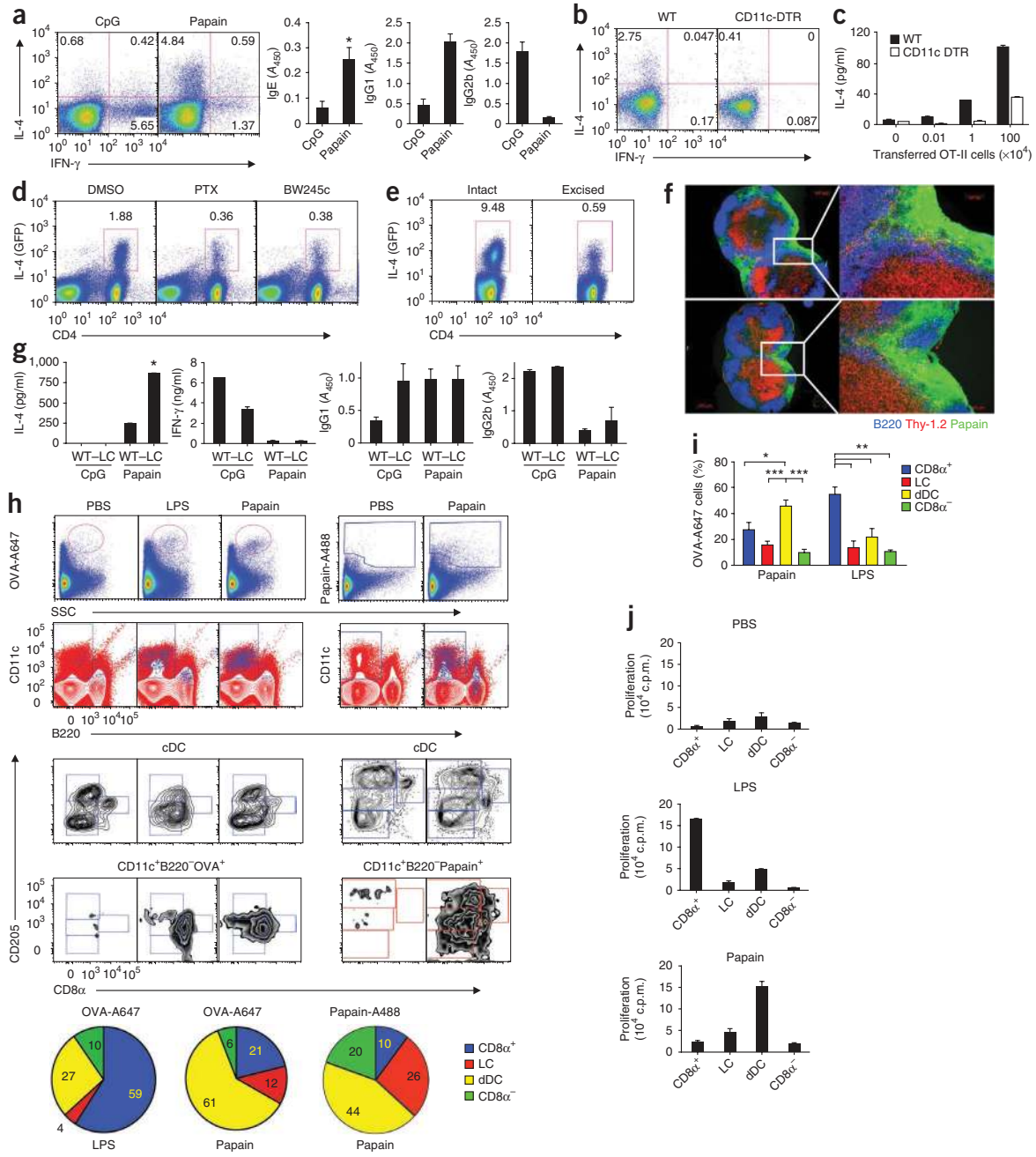

Figure 1 Vital role of DCs in papain-induced T_H2 responses. (**a**) Intracellular staining of IL-4 and IFN-γ in CD4+ T cells (left; day 21) and anti-OVA IgE, IgG1 and IgG2b in serum (right; day 21) from mice immunized on days 0, 7 and 14 with CpG or papain. A_{450}, absorbance at 450 nm. (**b**) Intracellular staining of IFN-γ and IL-4 in CD4+ T cells from DC-depleted wild-type (WT) and CD11c-DTR mice immunized 4 d earlier with OVA plus papain. Numbers in quadrants (**a**,**b**) indicate percent cells in each. (**c**) ELISA of IL-4 in supernatants of draining lymph node cells from wild-type or CD11c-DTR mice given various numbers of CD4+ OT-II T cells 24 h before diphtheria toxin treatment, then immunized with OVA plus papain; 4 d later, cells were restimulated for 4 d *ex vivo* with OVA peptide (amino acids 323–339). (**d**) IL-4-producing CD4+ T cells from 4get mice given no pretreatment (dimethyl sulfoxide (DMSO)) or pretreated with pertussis toxin (PTX) or BW245c, then immunized with OVA plus papain; IL-4 was assessed 4 d later as green fluorescent protein (GFP). (**e**) IL-4-producing CD4+ T cells 4 d after immunization with OVA plus papain, with the site of immunization excised 6 h after immunization. Numbers above outlined areas (**d**,**e**) indicate percent IL-4+CD4+ T cells. (**f**) Immunofluorescence microscopy of frozen sections of draining lymph nodes ($n = 2$) from mice 2 h after injection of Alexa Fluor 488–labeled papain (green). Blue, B220 (B cell–associated marker); red, Thy-1.2 (CD90.2); right, enlargement of area outlined at left. Original magnification, ×5 (left) or ×20 (right). (**g**) Production of IL-4 and IFN-γ by CD4+ T cells (left) and anti-OVA IgG1 and IgG2b in serum (right; day 14) from wild-type mice and Langerhans cell–depleted langerin-DTR mice (–LC) after immunization with OVA plus papain, as described in **a**. *, $P < 0.05$ (*t*-test). (**h**) Uptake of OVA or papain by DC subsets (identified and defined as described in Results) in draining lymph nodes isolated from mice 24 h after subcutaneous immunization with Alexa Fluor 647–labeled OVA (OVA-A647) plus papain, or Alexa Fluor 488–labeled papain (Papain-A488) alone. Bottom, proportion of fluorescence-labeled cells in conventional DC (cDC) subsets. SSC, side scatter; LC, Langerhans cell; dDC, dermal DC. (**i**) Pooled data from **h**. (**j**) Immunostimulatory capacity of the four lymph node DC subsets sorted by flow cytometry from mice immunized 24 h earlier with OVA plus papain or OVA plus LPS, then cultured with OT-II CD4+ T cells; proliferation was assessed by thymidine labeling. *$P < 0.05$, **$P < 0.01$ and ***$P < 0.001$ (analysis of variance). Data are representative of three to five independent experiments (mean and s.e.m.).

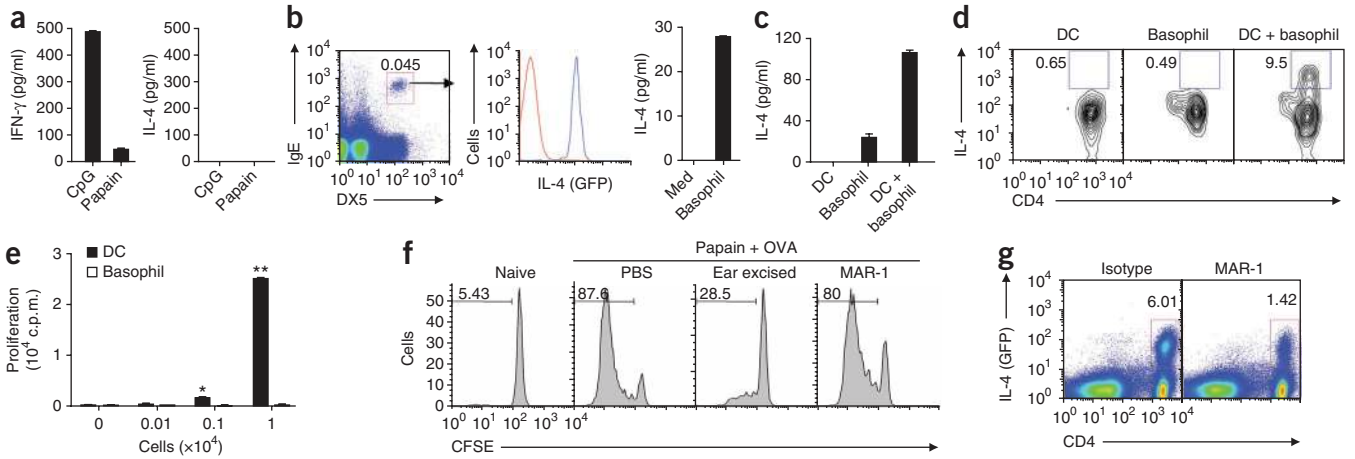

Figure 2 DCs and basophils act in concert to drive T_H2 responses. (**a**) Production of IFN-γ and IL-4 by OT-II $CD4^+$ T cells after culture with $CD11c^+$ lymph node DCs from mice immunized 24 h before with OVA plus papain or OVA plus CpG. (**b**) Flow cytometry analysis of IL-4 expression (middle) by IgE^+DX5^+ basophils (blue line) and nonbasophils (red line) sorted (left) from draining lymph nodes of 4get mice immunized subcutaneously 3 d earlier with papain, and ELISA of IL-4 production by flow cytometry–sorted basophils from mice immunized subcutaneously with papain plus OVA (right). Med, well with medium only. Number above outlined area (left) indicates percent IgE^+DX5^+ cells. (**c**) IL-4 production by cocultures of OT-II $CD4^+$ T cells and $CD11c^+$ DCs, basophils or a combination of DCs plus basophils isolated from mice immunized with OVA plus papain. (**d**) Intracellular flow cytometry analysis of IL-4-producing OT-II $CD4^+$ T cells cultured as in **c**. Numbers adjacent to outlined areas indicate percent $IL\text{-}4^+CD4^+$ cells. (**e**) Proliferation of OT-II $CD4^+$ T cells stimulated *in vitro* with various numbers of lymph node $CD11c^+$ DCs or basophils isolated from mice immunized with OVA plus papain, with no exogenous OVA added, assessed by [^{3}H]thymidine incorporation. (**f**) Proliferation of OT-II cells (labeled with the cytosolic dye CFSE) from unimmunized mice (Naive) or mice immunized with OVA plus papain and assessed with no further treatment (PBS), after ablation of skin-derived DCs by ear excision 6 h after immunization, or after depletion of basophils with MAR-1. Numbers above bracketed lines indicate percent $CSFE^+$ (dividing) cells. (**g**) Flow cytometry analysis of IL-4 expression in $CD4^+$ T cells in 4get mice, assessed (as green fluorescent protein) after basophil depletion and immunization as in **f**. Numbers above outlined areas indicate percent $IL\text{-}4^+CD4^+$ cells. $^*P < 0.05$ and $^{**}P < 0.01$ (*t*-test). Data are representative of three independent experiments (error bars (**a**–**c**,**e**), s.e.m.).

cells together with naive OT-II T cells *in vitro*. We assessed the proliferation of OT-II T cells by incorporation of tritiated thymidine ([^{3}H]thymidine). Dermal DCs, but not $CD8\alpha^+$ DCs, Langerhans cells or $CD8\alpha^-$ DCs, isolated from mice immunized with papain plus OVA induced robust proliferation of OT-II T cells; this was consistent with uptake of antigen (**Fig. 1h**,**j**). However, in mice immunized with LPS plus OVA, the proliferation of OT-II cells was induced mainly by $CD8\alpha^+$ DCs, which was again consistent with uptake of antigen (**Fig. 1h**,**j**). In summary, dermal DCs, but not Langerhans cells, have an essential role in the uptake and presentation of papain and OVA that results in robust antigen-specific T_H2 responses in mice.

Cooperation between DCs and basophils

To investigate whether DCs were sufficient to induce T_H2 differentiation in response to papain *in vivo*, we subcutaneously mice immunized with OVA plus papain or OVA plus CpG. We collected draining lymph nodes 24 h after immunization, digested the nodes and isolated $CD11c^+$ DCs by flow cytometry sorting. We cultured DCs for 72 h together with OVA-specific T cells from OT-II mice to examine the induction of T cell differentiation. DCs isolated from mice immunized with CpG plus OVA induced robust T_H1 cytokine responses characterized by the production of IFN-γ without detectable IL-4 (**Fig. 2a**). Although, as shown above (**Fig. 1j**), DCs isolated from mice immunized with OVA plus papain were able to induce the proliferation of OT-II cells, they failed to induce IL-4 production. These experiments suggested the involvement of accessory cells in the induction of a T_H2 response to papain. Studies have suggested that basophils are critically involved in the induction of T_H2 in response to protease allergens and infection with helminths[14–16,26]. Basophils can be recruited to lymph nodes in response to challenge with papain[15,26]. To determine whether basophils and DCs have a shared role in T_H2 immunity to papain, we isolated both cell subsets from lymph nodes of mice subcutaneously immunized with OVA plus papain. We purified DCs 22 h after immunization, as DC migration was first apparent at that time point[15,26]. Recruitment of basophils to the draining lymph nodes is known to peak at day 3 after immunization[15,26]. We found that basophils produced IL-4 (**Fig. 2b**). We isolated DCs and basophils from mice immunized with OVA plus papain and cultured naive OT-II helper T cells *in vitro* with DCs, basophils, or a combination of DCs and basophils. We collected cell culture supernatants at 5 d and analyzed IL-4 production. Consistent with our data above (**Fig. 2a**), we detected no IL-4 in the supernatants of T cells cultured with DCs (**Fig. 2c**). We observed moderate concentrations of IL-4 in the supernatants of T cells cultured with basophils and substantial enhancement of IL-4 production (about fivefold) for T cells cultured with both DCs and basophils. To confirm those findings and to establish the finding of production of IL-4 by OT-II $CD4^+$ T cells, we did intracellular staining for IL-4. We detected very few IL-4-producing T cells when we cultured OT-II T cells together with DCs alone (**Fig. 2d**). This demonstrates that DCs are insufficient to polarize a T_H2 response after stimulation with papain. Furthermore, there was no IL-4 production in T cells cultured with basophils alone, although we detected small amounts of IL-4 cytokine in the culture supernatants by enzyme-linked immunosorbent assay (ELISA). Notably, $CD4^+$ T cells cultured with both DCs and basophils produced IL-4 (**Fig. 2d**). Together, these data demonstrate that DCs or basophils alone are unable to stimulate T_H2 responses to papain; instead, they act in concert to promote antigen-specific T_H2 differentiation.

Basophils respond to papain by migrating to lymph nodes and producing T_H2-inducing cytokines *in vivo* as described before[15,26] and as shown here (**Fig. 2b**). Basophils express major histocompatibility complex class II molecules[14–16] and costimulatory molecules[14,15]

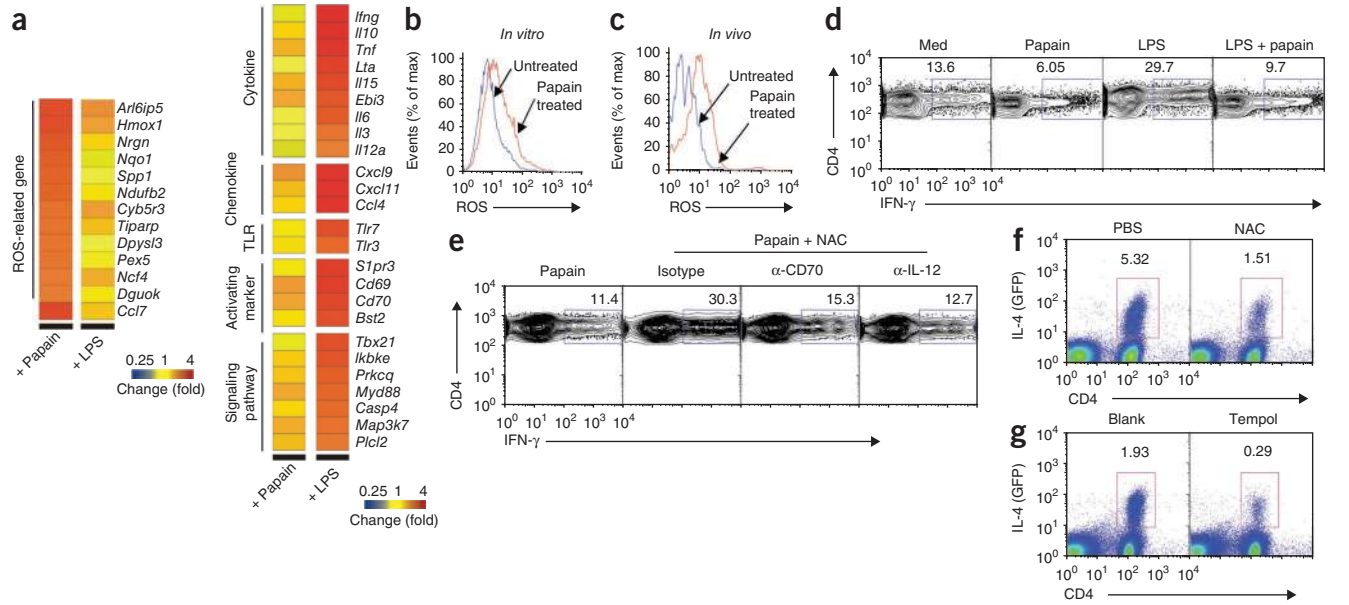

Figure 3 ROS production by papain-activated DCs is critical for T_H2 differentiation. (**a**) Microarray analysis of gene expression in lymph node DCs stimulated for 4 or 17 h *in vitro* with papain or LPS. (**b**,**c**) Flow cytometry analysis of ROS production by untreated and papain-stimulated DCs *in vitro* (**b**) and *in vivo* (**c**). (**d**) Flow cytometry analysis of intracellular IFN-γ production by OT-II T cells stimulated for 72 h with lymph node DCs pulsed with OVA peptide, amino acids 323–339, alone (Med) or together with papain, LPS, or LPS plus papain. (**e**) IFN-γ production assessed as in **d** but for cells pulsed with papain alone (far left) or with papain plus NAC in the presence of neutralizing anti-CD70 (α-CD70) or anti-IL-12 (α-IL-12) or isotype-matched control antibody (Isotype). (**f**,**g**) Flow cytometry analysis of IL-4 expression (as green fluorescent protein) in $CD4^+$ T cells from draining lymph nodes of 4get mice immunized with papain, with no pretreatment (PBS (**f**) or Blank (**g**)) or after pretreatment with NAC (**f**) or microparticle-encapsulated tempol (**g**). Numbers above outlined areas indicate percent $CD4^+IFN\text{-}\gamma^+$ cells (**d**,**e**) or $IL\text{-}4^+CD4^+$ cells (**f**,**g**). Data are representative of one experiment (**a**) or two to five experiments (**b**–**g**).

and can endocytose soluble proteins *in vitro*[15]. Yet basophils were unable to promote a T_H2 response in the absence of DCs *in vivo*. IL-4 expression in T cells is thought to be dependent on the cell cycle, with at least three cell divisions being required[37]. We hypothesized that basophils may not be able to present antigen to T cells or stimulate T cell proliferation *in vivo*. To establish the role of basophils in the ability to stimulate the proliferation of antigen-specific $CD4^+$ T cells, we assayed [^{3}H]thymidine incorporation in antigen-specific $CD4^+$ T cells cultured with either basophils sorted by flow cytometry or DCs from draining lymph nodes. Basophils did not stimulate T cell proliferation, whereas DCs stimulated robust proliferation of $CD4^+$ T cells (**Fig. 2e**). Even in the presence of exogenous OVA in the culture system, basophils showed much less antigen-presentation ability than did DCs (**Supplementary Fig. 7**). Therefore, the failure of basophils to prime a T_H2 response after immunization with OVA plus papain was most probably due to their inability to stimulate T cell proliferation. Consistent with those findings, we observed no change in T cell proliferation after depletion of basophils *in vivo* with the MAR-1 antibody to FcεRIα (anti-FcεRIα)[10] (**Fig. 2f** and **Supplementary Fig. 8**), although IL-4 production by $CD4^+$ T cells was much lower (**Fig. 2g**), consistent with published reports[26]. T cells proliferated less when we blocked the migration of DCs by surgical excision of the site of injection (**Fig. 2f**). These data demonstrate that DCs or basophils alone are insufficient to polarize a papain-induced T_H2 response. The 'cooperation' between these two cell types suggests a role for DCs in inducing T cell proliferation and a role for basophils in providing the IL-4 cytokine required for T_H2 differentiation in response to papain.

ROS and T_H2 responses to papain

To obtain insight into the molecular mechanism by which papain induced T_H2 responses, we first analyzed the cytokine responses of lymph node DCs stimulated with papain. Notably, papain-stimulated DCs did not produce detectable amounts of several pro- and anti-inflammatory mediators, as measured by multiplex bead analysis (**Supplementary Fig. 9**). We then assessed by microarray analysis changes in gene expression in lymph node DCs cultured *in vitro* with papain or LPS. We found upregulation of 447 or 567 genes by stimulation with papain or LPS, respectively, relative to expression without stimulus (medium only). LPS-activated DCs had higher expression of several T_H1-related genes, including *Il12a*, *Ebi3* (encoding IL-27), *Ifng*, *Cd70* and *Tbx21* (encoding the transcription factor T-bet; **Fig. 3a**). Notably, a group of ROS-related genes were upregulated after papain stimulation (**Fig. 3a**), including *Hmox1* (encoding HO-1) and *Ncf4* (encoding p40phox). HO-1 is recognized as a sensitive and reliable indicator of cellular oxidative stress, and p40phox is a subunit of the NADPH complex[38].

To confirm the production of ROS by DCs, we obtained lymph node DCs activated *in vitro* with papain or DCs from lymph nodes of papain-immunized mice and stained cells with the fluorescent dye DCF. We detected the production of ROS, as indicated by an increase in DCF fluorescence (**Fig. 3b**,**c**). The presence of ROS is recognized as an endogenous signal for the induction of inflammation, acute lung injury and artherosclerosis[39,40]. Although the role of ROS in asthma has been well documented[41], the involvement of ROS in induction of T_H2 responses to cysteine proteases is unknown at present. However, the production of ROS by macrophages diminishes their capacity to stimulate T_H1 responses[42]. We therefore determined whether ROS 'programmed' papain-induced DCs to stimulate T_H2 responses *in vitro*. OVA-pulsed DCs induced the T_H1 differentiation of OT-II cells *in vitro* (**Fig. 3d**). In contrast, the T_H1 response was enhanced by stimulation of DCs with LPS, a T_H1-polarizing stimulus. Notably, papain suppressed the ability of DCs to stimulate IFN-γ production.

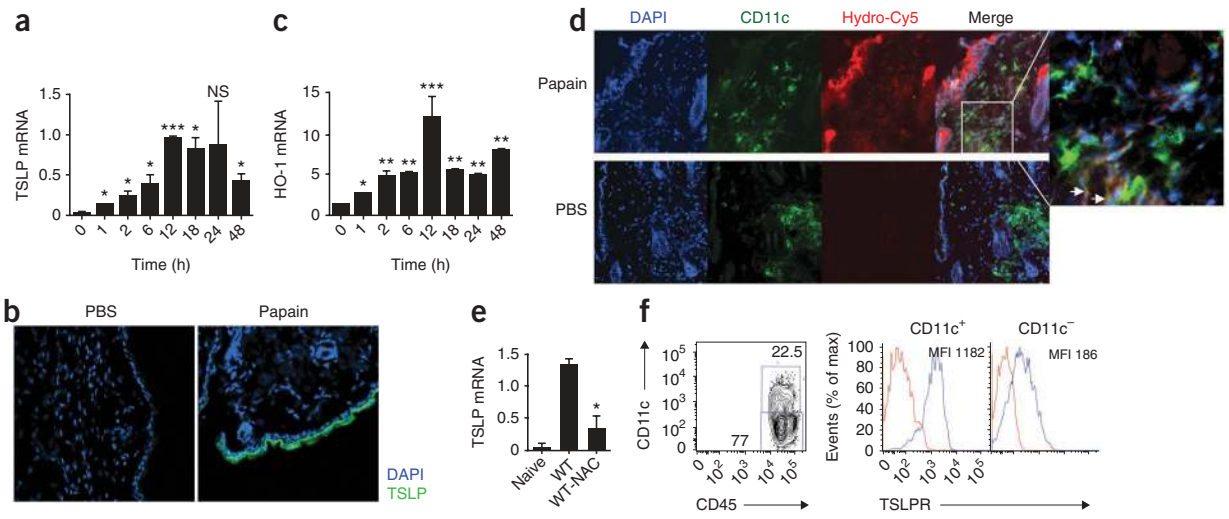

Figure 4 TSLP production in skin in response to immunization with papain is dependent on ROS. (**a**) Quantitative RT-PCR analysis of TLSP mRNA expression in ears of mice injected with papain, presented relative to the expression of GAPDH mRNA ('housekeeping' gene encoding glyceraldehyde phosphate dehydrogenase). (**b**) Immunofluorescence confocal microscopy of frozen ear sections from mice immunized with OVA plus papain. Blue, DAPI (DNA-intercalating dye); green, TSLP. Original magnification, ×20. (**c**) Quantitative RT-PCR analysis of HO-1 mRNA expression in ears of mice injected with papain, presented relative to GAPDH mRNA expression. (**d**) Immunofluorescence confocal microscopy of the site of immunization with OVA plus papain, stained for DAPI (blue), hydro-Cy5 (red) and CD11c (green) to assess ROS activity. Far right, enlargement of area outlined at left; arrows indicate some hydro-Cy5 staining in DCs. Original magnification, ×20 (main images). (**e**) Quantitative RT-PCR analysis of TSLP mRNA expression in ears of mice injected with papain, with (WT-NAC) or without (WT) pretreatment with NAC, presented relative to GAPDH mRNA expression. (**f**) Flow cytometry analysis of expression of the TSLP receptor (TLSPR; blue lines) on $CD11c^+$ and $CD11c^-$ dermal hematopoietic cells (sorted as shown at left), including dermal DCs. Red lines, isotype-matched control antibody. Numbers adjacent to outlined areas (left) indicate percent $CD11c^+CD45^+$ cells (top) or $CD11c^-CD45^+$ cells (bottom); MFI (right), mean fluorescent intensity. NS, not significant; $^*P < 0.05$, $^{**}P < 0.01$ and $^{***}P < 0.001$ (*t*-test). Data are representative of two to three independent experiments (error bars (**a**,**c**,**e**), s.e.m.).

Furthermore, the increase in the T_H1 response stimulated by LPS was decreased by culture of DCs with papain (**Fig. 3d**). We then determined whether ROS produced by papain-activated DCs were involved in the suppression of T_H1 differentiation. Blocking ROS by *N*-acetyl-cysteine (NAC), a ROS-specific inhibitor, restored the IFN-γ production suppressed by papain (**Fig. 3e**). IL-12 is a key cytokine in directing the development of T_H1 cells[2–5,43]. An IL-12-independent but CD70-dependent pathway of DC-mediated T_H1 polarization has been described[44]. We thus determined whether blocking ROS with NAC enhanced the expression of CD70 and IL-12p70 by DCs and found that it did (**Supplementary Fig. 10**). To further confirm that the T_H1 response restored by NAC was due to enhanced IL-12 or CD70, we added neutralizing antibody to IL-12 or CD70 to the *in vitro* cocultures. Neutralization of either CD70 or IL-12 resulted in a lower frequency of IFN-γ-producing T cells (**Fig. 3e**). These results suggest that the inhibition of T_H1 responses in DCs treated with papain is mediated by the production of ROS, which in turn suppresses the expression of CD70 or IL-12.

To assess the involvement of ROS in papain-mediated T_H2 responses *in vivo*, we injected 4get mice with PBS or NAC, then immunized the mice with OVA plus papain. At 4 d after immunization, we examined the production of IL-4 in $CD4^+$ T cells by flow cytometry. IL-4 production was much lower in mice treated with NAC (**Fig. 3f**), which indicated that ROS is critical in the induction of T_H2 responses by papain. To 'preferentially' target ROS inhibitors to phagocytic cells, including DCs[45], we encapsulated the hydrophobic ROS inhibitor tempol in biodegradable poly(ketal)-based microparticles[46] and treated mice with this before immunizing them with OVA plus papain. In mice injected with microparticle-encapsulated tempol before immunization, there was considerable inhibition of T_H2 responses (**Fig. 3g**). Similarly, inhibition of ROS also impaired T_H2 responses induced by the related cysteine protease bromelain (**Supplementary Fig. 11**). Together, these results demonstrate that ROS produced in cysteine protease–activated DCs is critical for the suppression of T_H1 responses and enhancement of T_H2 differentiation.

Papain-induced TSLP production

TSLP has a key role in the induction of T_H2 responses[47,48]. To investigate the role of TSLP in papain-induced T_H2 responses, we isolated RNA from the skin at the site of injection and from lymph node DCs at various time points (1, 2, 6 and 18 h) after immunization with papain. We first assessed TSLP mRNA by real-time PCR. We detected no TSLP mRNA in lymph node DCs (data not shown). However, in the skin, TSLP mRNA was induced by papain stimulation (**Fig. 4a**). Protein expression of TSLP, assessed by immunofluorescence staining of skin cryosections, was predominantly in the epidermis (**Fig. 4b**).

ROS are produced by epithelial cells[38]. We thus analyzed the presence of ROS at the site of injection. *Hmox1* expression has been used as a marker of intracellular oxidative stress[38]. We assessed *Hmox1* expression in skin by quantitative real-time PCR. We observed robust induction of HO-1 mRNA in skin at the site of injection with papain (**Fig. 4c**). We detected HO-1 mRNA expression as early as 1 h after papain injection; it peaked at 12 h and lasted for at least 48 h. The hydrocyanine dye hydro-Cy5 is a membrane-permeable molecule that, after oxidation with ROS, is modified into a membrane-impermeable dye, which allows accumulation of the dye in cells producing ROS[49]. We treated mice with papain for 6 h and then injected them with hydro-Cy5 at the same injection site 1 h before excising skin for staining. We excised skin from the injection site and costained it for CD11c to delineate the presence of ROS in epithelial cells. We detected robust ROS production mainly in epithelial cells, with a weak signal in $CD11c^+$ DCs in the dermis (**Fig. 4d**). Finally, we determined

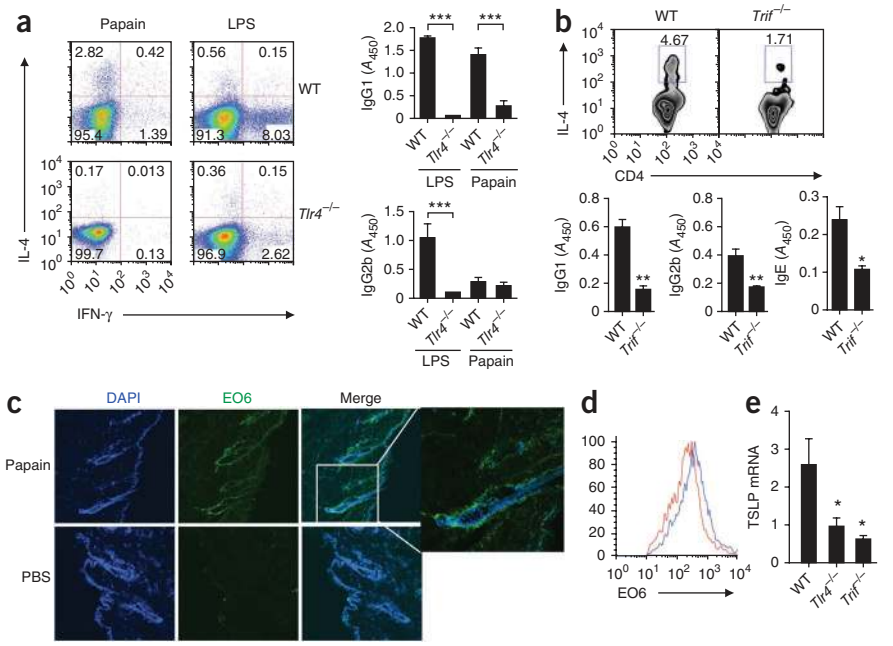

Figure 5 Papain-induced T_H2 responses are dependent on TLR4-TRIF signaling. (**a**) Flow cytometry of intracellular staining for IL-4 and IFN-γ in $CD4^+$ T cells from draining lymph nodes (left) and OVA-specific antibody titers (right) of wild-type or *Tlr4*$^{-/-}$ mice immunized with OVA plus papain or OVA plus LPS. Numbers in quadrants (left) indicate percent cells in each. (**b**) Flow cytometry of intracellular IL-4 staining in $CD4^+$ T cells from draining lymph nodes (above) and OVA-specific antibody titers (below) of wild-type and *Trif*$^{-/-}$ mice immunized as in **a**. Numbers above outlined areas (top) indicate percent IL-4$^+$CD4$^+$ cells. (**c**) Immunofluorescence microscopy of frozen tissue sections of skin at the site of immunization, obtained from C57BL/6 mice injected with PBS or papain, fixed and stained with the EO6 antibody specific for OxPLs. Far right, enlargement of area outlined at left. Original magnification, ×20 (main images). (**d**) Flow cytometry analysis of the expression of OxPLs in draining lymph node $CD11c^+$ DCs from mice injected with PBS (red line) or papain (blue line). (**e**) Quantitative RT-PCR analysis of TSLP mRNA expression in skin tissue derived from the site of immunization of papain-injected wild-type, TLR4-deficient or TRIF-deficient mice, presented relative to GAPDH mRNA expression. $^*P < 0.05$, $^{**}P < 0.01$ and $^{***}P < 0.001$ (*t*-test). Data are representative of two to three independent experiments (error bars (**a**,**b**,**e**), s.e.m.).

whether the expression of TSLP was ROS dependent. Real-time PCR data indicated that TSLP expression was significantly lower in NAC-treated mice (**Fig. 4e**). Also, we detected higher expression of TSLP receptor mRNA on DCs in the dermis (**Fig. 4f**) and $CD4^+$ T cells in lymph node (**Supplementary Fig. 12**). These data indicate a role for ROS in the induction of TSLP in epithelial cells that might in turn induce signaling in dermal DCs via the TSLP receptor as well as in $CD4^+$ T cells in draining lymph nodes, thereby promoting T_H2 differentiation[47,48].

The TLR4-TRIF signaling axis

Very little is known about the role of PRRs in the induction of T_H2 responses. We observed that papain-induced T_H2 responses were independent of signaling via TLR2, TLR3, TLR6, TLR7 or TLR9 (**Supplementary Fig. 13**). In addition, neither the Nod-like receptors NALP3 and IPAF nor their downstream signaling adaptor proteins, such as ASC and caspase-1, were required for the induction of T_H2 responses to papain (**Supplementary Fig. 14**). However, IL-4 production by $CD4^+$ T cells, as well as the production of OVA-specific IgG1 antibodies, were significantly lower in *Tlr4*$^{-/-}$ mice after immunization with OVA plus papain ($P < 0.05$). In contrast, the induction of T_H1 responses to OVA plus LPS was dependent on TLR4 (**Fig. 5a**). These data demonstrate that T_H2 induction by papain is dependent on TLR4 signaling. To eliminate endotoxin contamination, we used endotoxin-free OVA in these experiments, and in addition, we used polymixin B to neutralize any endotoxin. Treatment with polymyxin B did not alter the IL-4 production by $CD4^+$ T cells (**Supplementary Fig. 15**), which suggested that the T_H2-inducing effect of papain was not caused by endotoxin contamination. Furthermore, IL-4 production by $CD4^+$ T cells in 4get mice was much lower after stimulation with heat-inactivated papain (**Supplementary Fig. 15**), which indicated a role for the intrinsic enzymatic activity of papain in the induction of T_H2 responses. T_H2 responses were also significantly higher in mice deficient in the adaptor MyD88 ($P < 0.05$; **Supplementary Fig. 16**). In contrast, mice deficient in TRIF signaling showed much less production of IL-4 by $CD4^+$ T cells, as well as less OVA-specific IgG1 and IgE (**Fig. 5b**). As both MyD88 and TRIF are necessary for endotoxin signaling, it is unlikely that the papain-induced T_H2 responses were due to endotoxin contamination. Collectively, these data demonstrate that TLR4-TRIF signaling is involved in T_H2 immunity induced by papain, but they raise questions about the nature of the ligand that initiates signaling via TLR4. One clue came from experiments demonstrating that induction of HO-1 was independent of TLR4 (data not shown). However, oxidized moieties, including oxidized phospholipids (OxPLs), can activate TLR4 on macrophages[39,40,50,51], and ROS can induce the formation of OxPLs, which signal via the TLR4-TRIF-dependent pathway[40]. We thus hypothesized that the induction of ROS by papain could lead to the formation of OxPLs. The monoclonal antibody EO6 is specific to OxPLs and distinguishes them from nonoxidized phospholipids[40]. We observed considerable EO6-stained OxPLs in skin epithelial cells by immunofluorescence staining (**Fig. 5c**). In addition, flow cytometry analysis demonstrated the generation of EO6-detectable OxPLs in papain-activated DCs in draining lymph nodes (**Fig. 5d**). These data demonstrate that ROS generated by stimulation with papain triggers the oxidative-stress machinery and the production of OxPLs in skin and in draining lymph nodes. Furthermore, consistent with published studies of OxPLs[39], we observed phosphorylation of the ubiquitin ligase TRAF6 in papain-treated DCs (data not shown). Together, our results indicate a link among ROS, OxPLs and TLR4- and TRIF-based signaling in the induction of T_H2 responses after stimulation with papain. Furthermore, the induction of TSLP in skin was also tightly regulated by TLR4 and TRIF signaling (**Fig. 5e**).

Recruitment of basophils to lymph nodes

As described above (**Fig. 2c–e**), the recruitment of basophils to draining lymph nodes is critical in papain-induced T_H2 responses. Microarray analysis showed that CCL7 (MCP-3), a basophil-attracting chemokine[52], was selectively upregulated in papain-stimulated lymph node DCs but not in LPS-stimulated DCs (**Fig. 3a**). We further

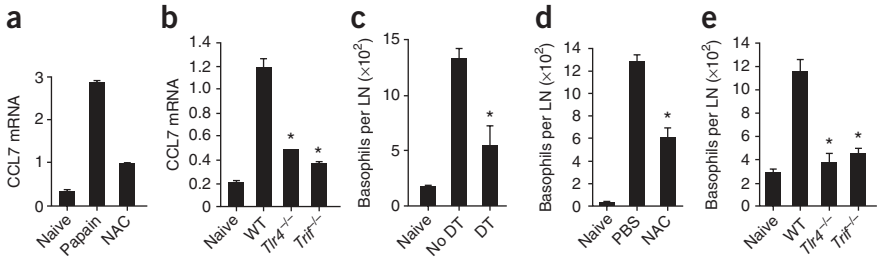

Figure 6 Regulation of basophil migration by ROS, TLR4 and TRIF signaling in DCs. (**a**) RT-PCR analysis of CCL7 mRNA expression by lymph node DCs isolated from unimmunized mice (Naive; left) or mice immunized subcutaneously with papain with (right) or without (middle) NAC pretreatment. (**b**) CCL7 mRNA expression by lymph node DCs from wild-type, TLR4-deficient or TRIF-deficient mice left unimmunized or immunized with papain. Results in **a**,**b** are presented relative to GAPDH mRNA expression. (**c**) Recruitment of basophils to the lymph nodes in CD11c-DTR mice left undepleted (no DT) or depleted of DCs (DT) and then immunized subcutaneously 1 d later with papain and evaluated 3 d later. LN, lymph node. (**d**) Recruitment of basophils to the lymph nodes in wild-type mice immunized with papain, with (NAC) or without (PBS) pretreatment with NAC. (**e**) Recruitment of basophils to the lymph nodes in unimmunized mice and wild-type, *Tlr4*$^{-/-}$ and *Trif*$^{-/-}$ mice immunized with papain. *$P < 0.05$ (*t*-test). Data are representative of two to three independent experiments.

confirmed higher CCL7 mRNA expression by real-time PCR in lymph node–resident DCs activated by papain *in vivo*. Moreover, as described earlier for TSLP, the production of CCL7 by DCs was tightly regulated by the ROS, TLR4 and TRIF signaling pathways (**Fig. 6a**,**b**). We further hypothesized that activation of lymph node DCs by papain greatly increased secretion of CCL7, which subsequently recruited basophils to the draining lymph nodes to support T_H2 responses. To test our hypothesis, we ablated DCs in CD11c-DTR mice by injection of diphtheria toxin and quantified the migration of basophils to the draining lymph nodes. The absolute number of basophils in draining lymph nodes was significantly lower after depletion of DCs (**Fig. 6c**), which suggests that DCs are critical in attracting basophils to lymph nodes. In contrast, we did not find significantly fewer basophils in draining lymph node after depletion of T cells through the use of anti-CD3 ($P > 0.1$; **Supplementary Fig. 17**), which indicated that T cells did not have a role in the recruitment of basophils. Next, we evaluated the migration of basophils after treatment with NAC (ROS blockade) and in *Tlr4*$^{-/-}$ and *Trif*$^{-/-}$ mice. The migration of basophils to draining lymph nodes was significantly less after treatment with NAC (**Fig. 6d**). Furthermore, we observed significantly fewer basophils in *Tlr4*$^{-/-}$ and *Trif*$^{-/-}$ mice than in wild-type mice in response to immunization with papain (**Fig. 6e**). Our data suggest that papain-activated DCs efficiently recruit basophils to draining lymph nodes and indicate a role for the DC-derived chemokine CCL7 in attracting basophils. Furthermore, ROS, TLR4 and TRIF signaling were critical in the induction of CCL7 in papain-stimulated DCs. Together, these results demonstrate that T_H2 responses to papain are orchestrated by ROS-dependent TLR4-TRIF signaling, which mediates the concerted action of DCs and basophils (**Supplementary Fig. 18**).

Optimal T_H2 induction

Papain induced IL-4 in basophils[15] (**Fig. 2a**) and TSLP in epithelial cells[15] (**Fig. 4a**,**b**) and also suppressed IL-12 production in DCs and directly inhibited their ability to stimulate T_H1 responses (**Fig. 3** and **Supplementary Fig. 10**). We determined the relative importance of IL-4, TSLP and suppression of IL-12 in T_H2 induction by papain. First we did an experiment *in vivo* to neutralize both IL-4 and TSLP, as well as to supplement IL-12. We reconstituted *Il4*$^{-/-}$ mice on day −1 with OT-II CD4$^+$ T cells and injected the mice on day 0 subcutaneously with anti–mouse TSLP and intraperitoneally with recombinant mouse IL-12, then immunized them 2 h later with OVA plus papain. We injected wild-type mice with isotype-matched control antibody at the same time and immunized them with OVA plus papain. On days +2 and +3, we injected mice again with anti-TSLP and also injected them with IL-12 on days +1, +2 and +3. On day +4, we isolated lymph node cells and restimulated them for 5 h *in vitro* on plates precoated with anti-CD3 and anti-CD28 in the presence of GolgiStop. We then analyzed IL-4 production by intracellular flow cytometry staining. We observed a lower frequency of IL-4$^+$ CD4$^+$ T cells (**Supplementary Fig. 19a**). To determine the relative contributions of IL-4 and TSLP to this result, we did an independent experiment in which we immunized wild-type and *Il4*$^{-/-}$ mice injected with anti-TSLP, as well as uninjected wild-type and *Il4*$^{-/-}$ mice, with OVA plus papain (**Supplementary Fig. 19b**). We then evaluated the antigen-specific CD4$^+$ T cell response as described above. Blockade of either IL-4 or TSLP alone resulted in T_H2 responses only modestly lower than those of mice that received isotype-matched control antibodies (**Supplementary Fig. 19b**); this result was consistent with published work[15]. In contrast, combined blockade of TSLP and IL-4 resulted in a more pronounced effect (**Supplementary Fig. 19b**). Together, these findings demonstrate that papain-mediated induction of IL-4 and TSLP, along with the suppression of IL-12, creates a permissive environment for the optimal induction of T_H2 responses (**Supplementary Fig. 18**).

DISCUSSION

The role of DCs in the induction of T_H2 responses has been addressed before[22–25]. However, the role of DCs in the induction of T_H2 immunity to allergens has been challenged by a study reporting that DCs are neither sufficient nor essential for the induction of T_H2 responses to papain[15]. The finding that DCs were not essential was demonstrated by ablation of DCs in lethally irradiated wild-type mice reconstituted with bone marrow derived from CD11c-DTR mice (chimeric mice)[27] and subsequently immunized with papain plus antigen[15]. In contrast, our results have indicated that depletion of DCs in CD11c-DTR mice through the use of diphtheria toxin abrogated the induction of T_H2 responses to papain plus antigen. Results obtained by excision of the site of injection, as well as blocking DC migration with inhibitors, supported the idea of a role for skin-derived migratory DCs in the induction of T_H2 responses. *In vitro* analysis of sorted DC subsets indicated the involvement of dermal DCs in the induction of antigen-specific proliferation of CD4$^+$ T helper cells in response to immunization with OVA plus papain. A possible explanation for the differences between our study here and the previously published study[15] may be explained by earlier work demonstrating that a substantial proportion of CD11c$^+$ cells in the dermis are resistant to depletion by irradiation[53]. Chimeric mice generated with CD11c-DTR bone marrow could potentially carry 25% residual dermal DCs derived from the host bone marrow (wild-type; CD11c-DTR$^-$) that cannot be depleted by treatment with diphtheria toxin and hence potentially contribute to the adaptive response. In addition, incomplete depletion of donor-derived DCs by diphtheria toxin could result in substantial numbers of dermal DCs that promote T_H2 responses. Furthermore, independent studies have demonstrated impairment of T_H2 responses after depletion of DCs in CD11c-DTR mice[25]. The previously published study[15]

further demonstrated that DCs are not sufficient for T_H2 responses to papain by using CD11c-Aβ^b mice[54,55], in which major histocompatibility complex class II is selectively expressed on CD11c$^+$ DCs; this is consistent with our results presented here.

The key DC-derived signals that mediate T_H2 immunity to allergens are still unclear. IL-4 and TSLP can initiate T_H2 responses, but our results have indicated that DCs do not produce such cytokines yet have a vital role in the induction of T_H2 responses. Basophils can migrate to draining lymph nodes in response to allergens or helminths[15,16,26] and secrete IL-4 and TSLP[26]. Furthermore, basophils express major histocompatibility complex class II as well as costimulatory molecules[15,16] and take up soluble antigen *in vitro* and can present antigens to T cells[15]. However, how efficiently they present antigens relative to antigen presentation by DCs is unclear. Our data have demonstrated that basophils from mice immunized with OVA plus papain were unable to stimulate efficient proliferation of CD4$^+$ T cells, even in the presence of exogenous OVA. Consistent with that finding, depletion of basophils *in vivo* by injection of MAR-1 (anti-FcεRIα) had no effect on T cell division, which demonstrates that basophils are not essential for the proliferation of antigen-specific CD4$^+$ T cells *in vivo*. Together, these data indicate a critical role for the concerted action of basophils and DCs in driving T_H2 immunity, with DCs providing antigen and basophils providing IL-4.

As for the molecular mechanisms by which cysteine proteases induce T_H2 responses, our results have demonstrated a key role for ROS. ROS generated by macrophages can suppress T_H1 responses[42]. Our results have shown that ROS suppress expression of IL-12 and CD70 in DCs, thereby favoring a T_H2 bias. *In vivo* suppression of ROS production in DCs, by targeting of an ROS inhibitor to DCs in microparticles, resulted in lower T_H2 responses. In addition to being generated by DCs, ROS were also generated by epithelial cells in response to papain immunization. TSLP, a cytokine known to be involved in T_H2 differentiation, is regulated in airway epithelial cells by the production of ROS[56]. In our studies, we observed that TSLP production in epithelial cells in response to papain at the site of injection was significantly lower after treatment with NAC, which suggests a role for ROS in modulating TSLP expression in epithelial cells in response to papain.

Finally, it is still unclear how helminths and allergens are sensed by innate immune cells. Few studies have attempted to study the role of PRRs in the response to helminths and allergens. Data indicate that in both airway epithelial cells and keratinocytes, PAR2 is an important protease-mediated mediator of TSLP expression[55,56]. Our preliminary data suggest that PAR-2 deficiency has a modest effect on papain-induced T_H2 responses (data not shown). In contrast, our results indicate that TLR4-mediated TRIF signaling is critical in papain-induced T_H2 responses. Studies have demonstrated that a TLR4-dependent, MyD88-independent pathway is critical in oxidative stress–related diseases[57]. It is unlikely that the TLR activation was due to endotoxin, for the following reasons: we used endotoxin-free OVA; polymixin B treatment did not affect T_H2 induction by OVA plus papain; T_H2 induction was significantly lower after immunization with heat-inactivated papain; the T_H2 response to papain was independent of MyD88, which is critical for endotoxin-mediated TLR4 triggering, and in fact, papain-induced T_H2 responses were greater in *Myd88*$^{-/-}$ mice; and the induction of HO-1 by papain was independent of TLR4 and TRIF (data not shown). Therefore, whichever TLR4 ligand was induced by papain must be downstream of HO-1. In this context, OxPLs can activate TLR4 (refs. 40,51), and our results indicated robust production of OxPLs in DCs and epithelial cells after stimulation with papain.

In summary, our data have demonstrated that T_H2 responses to cysteine proteases require DC-basophil 'cooperation' via ROS signaling. Cysteine proteases stimulate ROS production in DCs and epithelial cells. ROS have a central role in orchestrating T_H2 responses by inducing the formation of oxidized lipids that trigger TLR4-TRIF–mediated induction of TSLP by epithelial cells. In addition, ROS suppress production of the T_H1-inducing molecules IL-12 and CD70 in lymph node DCs and induce the DC-derived chemokine CCL7, thus facilitating the recruitment of IL-4$^+$ basophils to the lymph node.

METHODS

Methods and any associated references are available in the online version of the paper at http://www.nature.com/natureimmunology/.

Accession codes. GEO: microarray data, GSE21602.

Note: Supplementary information is available on the Nature Immunology website.

ACKNOWLEDGMENTS

We thank S.A. Mertens, L. Bronner and Y. Wang for assistance with cell sorting; Y. Wang, D. Levesque and D. Bonenberger for assistance with the maintenance of mice at the Emory Vaccine Center vivarium; S. Akira (Osaka University) for *Tlr2*$^{-/-}$, *Tlr3*$^{-/-}$, *Tlr4*$^{-/-}$, *Tlr6*$^{-/-}$, *Tlr7*$^{-/-}$, *Tlr9*$^{-/-}$, *Myd88*$^{-/-}$ and *Ticam1*$^{lps-2/lps-2}$ mice; V. Dixit (Genentech) for *Nalp3*$^{-/-}$, *Ipaf*$^{-/-}$ and *Asc*$^{-/-}$ mice; K.A. Hogquist (University of Minnesota) for Langerin-EGFP-DTR mice; and J. Witztum (University of California at San Diego) for EO6. Supported by the National Institutes of Health (U54AI057157, R37AI48638, R01DK057665, U19AI057266, HHSN266 200700006C, N01 AI50019, N01 AI50025) and the Bill & Melinda Gates Foundation.

AUTHOR CONTRIBUTIONS

H.T. and B.P. designed experiments; H.T. did experiments; R.R. and W.C. assisted with experiments; S.P.K. K.K. and N.M. designed microparticles and assisted with ROS imaging; T.B.K. and H.L.N. assisted with data analyses.; B.M. provided mice; and H.T. and B.P. wrote the manuscript.

COMPETING FINANCIAL INTERESTS

The authors declare no competing financial interests.

Published online at http://www.nature.com/natureimmunology/.
Reprints and permissions information is available online at http://npg.nature.com/reprintsandpermissions/.

1. Mosmann, T.R. & Coffman, R.L. TH1 and TH2 cells: different patterns of lymphokine secretion lead to different functional properties. *Annu. Rev. Immunol.* **7**, 145–173 (1989).
2. Zhu, J., Yamane, H. & Paul, W.E. Differentiation of effector CD4 T cell populations. *Annu. Rev. Immunol.* **28**, 445–489 (2010).
3. Korn, T., Bettelli, E., Oukka, M. & Kuchroo, V.K. IL-17 and Th17 Cells. *Annu. Rev. Immunol.* **27**, 485–517 (2009).
4. Steinman, R.M. & Banchereau, J. Taking dendritic cells into medicine. *Nature* **449**, 419–426 (2007).
5. Steinman, R.M. Dendritic cells in vivo: a key target for a new vaccine science. *Immunity* **29**, 319–324 (2008).
6. Heath, W.R. & Carbone, F.R. Dendritic cell subsets in primary and secondary T cell responses at body surfaces. *Nat. Immunol.* **10**, 1237–1244 (2009).
7. Kawai, T. & Akira, S. The role of pattern-recognition receptors in innate immunity: update on Toll-like receptors. *Nat. Immunol.* **11**, 373–384 (2010).
8. Urban, J.F. Jr. *et al.* The importance of Th2 cytokines in protective immunity to nematodes. *Immunol. Rev.* **127**, 205–220 (1992).
9. Khodoun, M.V., Orekhova, T., Potter, C., Morris, S. & Finkelman, F.D. Basophils initiate IL-4 production during a memory T-dependent response. *J. Exp. Med.* **200**, 857–870 (2004).
10. Denzel, A. *et al.* Basophils enhance immunological memory responses. *Nat. Immunol.* **9**, 733–742 (2008).
11. Galli, S.J., Nakae, S. & Tsai, M. Mast cells in the development of adaptive immune responses. *Nat. Immunol.* **6**, 135–142 (2005).
12. Min, B. & Paul, W.E. Basophils: in the spotlight at last. *Nat. Immunol.* **9**, 223–225 (2008).
13. Min, B. *et al.* Basophils produce IL-4 and accumulate in tissues after infection with a Th2-inducing parasite. *J. Exp. Med.* **200**, 507–517 (2004).
14. Yoshimoto, T. *et al.* Basophils contribute to T_H2-IgE responses in vivo via IL-4 production and presentation of peptide-MHC class II complexes to CD4$^+$ T cells. *Nat. Immunol.* **10**, 706–712 (2009).

15. Sokol, C.L. *et al.* Basophils function as antigen-presenting cells for an allergen-induced T helper type 2 response. *Nat. Immunol.* **10**, 713–720 (2009).
16. Perrigoue, J.G. *et al.* MHC class II-dependent basophil-CD4$^+$ T cell interactions promote T_H2 cytokine-dependent immunity. *Nat. Immunol.* **10**, 697–705 (2009).
17. Dillon, S. *et al.* A Toll-like receptor 2 ligand stimulates Th2 responses in vivo, via induction of extracellular signal-regulated kinase mitogen-activated protein kinase and c-Fos in dendritic cells. *J. Immunol.* **172**, 4733–4743 (2004).
18. Redecke, V. *et al.* Cutting edge: activation of Toll-like receptor 2 induces a Th2 immune response and promotes experimental asthma. *J. Immunol.* **172**, 2739–2743 (2004).
19. Eisenbarth, S.C. *et al.* Lipopolysaccharide-enhanced, Toll-like receptor 4-dependent T helper cell type 2 responses to inhaled antigen. *J. Exp. Med.* **196**, 1645–1651 (2002).
20. Yang, D. *et al.* Eosinophil-derived neurotoxin acts as an alarmin to activate the TLR2-MyD88 signal pathway in dendritic cells and enhances Th2 immune responses. *J. Exp. Med.* **205**, 79–90 (2008).
21. Fritz, J.H. *et al.* Nod1-mediated innate immune recognition of peptidoglycan contributes to the onset of adaptive immunity. *Immunity* **26**, 445–459 (2007).
22. Maldonado-Lopez, R. *et al.* CD8α^+ and CD8α^- subclasses of dendritic cells direct the development of distinct T helper cells in vivo. *J. Exp. Med.* **189**, 587–592 (1999).
23. Pulendran, B. *et al.* Distinct dendritic cell subsets differentially regulate the class of immune response in vivo. *Proc. Natl. Acad. Sci. USA* **96**, 1036–1041 (1999).
24. Kapsenberg, M.L. Dendritic-cell control of pathogen-driven T-cell polarization. *Nat. Rev. Immunol.* **3**, 984–993 (2003).
25. van Rijt, L.S. *et al.* In vivo depletion of lung CD11c$^+$ dendritic cells during allergen challenge abrogates the characteristic features of asthma. *J. Exp. Med.* **201**, 981–991 (2005).
26. Sokol, C.L., Barton, G.M., Farr, A.G. & Medzhitov, R. A mechanism for the initiation of allergen-induced T helper type 2 responses. *Nat. Immunol.* **9**, 310–318 (2008).
27. Jung, S. *et al.* In vivo depletion of CD11c$^+$ dendritic cells abrogates priming of CD8$^+$ T cells by exogenous cell-associated antigens. *Immunity* **17**, 211–220 (2002).
28. Allan, R.S. *et al.* Migratory dendritic cells transfer antigen to a lymph node-resident dendritic cell population for efficient CTL priming. *Immunity* **25**, 153–162 (2006).
29. Mohrs, M., Shinkai, K., Mohrs, K. & Locksley, R.M. Analysis of type 2 immunity in vivo with a bicistronic IL-4 reporter. *Immunity* **15**, 303–311 (2001).
30. Itano, A.A. *et al.* Distinct dendritic cell populations sequentially present antigen to CD4 T cells and stimulate different aspects of cell-mediated immunity. *Immunity* **19**, 47–57 (2003).
31. Kissenpfennig, A. *et al.* Dynamics and function of Langerhans cells in vivo: dermal dendritic cells colonize lymph node areas distinct from slower migrating Langerhans cells. *Immunity* **22**, 643–654 (2005).
32. Bursch, L.S. *et al.* Identification of a novel population of Langerin$^+$ dendritic cells. *J. Exp. Med.* **204**, 3147–3156 (2007).
33. Henri, S. *et al.* The dendritic cell populations of mouse lymph nodes. *J. Immunol.* **167**, 741–748 (2001).
34. Poulin, L.F. *et al.* The dermis contains langerin$^+$ dendritic cells that develop and function independently of epidermal Langerhans cells. *J. Exp. Med.* **204**, 3119–3131 (2007).
35. Ginhoux, F. *et al.* Blood-derived dermal langerin$^+$ dendritic cells survey the skin in the steady state. *J. Exp. Med.* **204**, 3133–3146 (2007).
36. Bedoui, S. *et al.* Cross-presentation of viral and self antigens by skin-derived CD103$^+$ dendritic cells. *Nat. Immunol.* **10**, 488–495 (2009).
37. Bird, J.J. *et al.* Helper T cell differentiation is controlled by the cell cycle. *Immunity* **9**, 229–237 (1998).
38. Bedard, K. & Krause, K.H. The NOX family of ROS-generating NADPH oxidases: physiology and pathophysiology. *Physiol. Rev.* **87**, 245–313 (2007).
39. Binder, C.J. *et al.* Innate and acquired immunity in atherogenesis. *Nat. Med.* **8**, 1218–1226 (2002).
40. Imai, Y. *et al.* Identification of oxidative stress and Toll-like receptor 4 signaling as a key pathway of acute lung injury. *Cell* **133**, 235–249 (2008).
41. Riedl, M.A. & Nel, A.E. Importance of oxidative stress in the pathogenesis and treatment of asthma. *Curr. Opin. Allergy Clin. Immunol.* **8**, 49–56 (2008).
42. Gelderman, K.A. *et al.* Macrophages suppress T cell responses and arthritis development in mice by producing reactive oxygen species. *J. Clin. Invest.* **117**, 3020–3028 (2007).
43. Abbas, A.K., Murphy, K.M. & Sher, A. Functional diversity of helper T lymphocytes. *Nature* **383**, 787–793 (1996).
44. Soares, H. *et al.* A subset of dendritic cells induces CD4$^+$ T cells to produce IFN-γ by an IL-12-independent but CD70-dependent mechanism in vivo. *J. Exp. Med.* **204**, 1095–1106 (2007).
45. Cao, W. *et al.* Toll-like receptor-mediated induction of type I interferon in plasmacytoid dendritic cells requires the rapamycin-sensitive PI(3)K-mTOR-p70S6K pathway. *Nat. Immunol.* **9**, 1157–1164 (2008).
46. Heffernan, M.J., Kasturi, S.P., Yang, S.C., Pulendran, B. & Murthy, N. The stimulation of CD8$^+$ T cells by dendritic cells pulsed with polyketal microparticles containing ion-paired protein antigen and poly(inosinic acid)-poly(cytidylic acid). *Biomaterials* **30**, 910–918 (2009).
47. Liu, Y.J. *et al.* TSLP: an epithelial cell cytokine that regulates T cell differentiation by conditioning dendritic cell maturation. *Annu. Rev. Immunol.* **25**, 193–219 (2007).
48. Ziegler, S.F. & Liu, Y.J. Thymic stromal lymphopoietin in normal and pathogenic T cell development and function. *Nat. Immunol.* **7**, 709–714 (2006).
49. Kundu, K. *et al.* Hydrocyanines: a class of fluorescent sensors that can image reactive oxygen species in cell culture, tissue, and in vivo. *Angew. Chem. Int. Edn Engl.* **48**, 299–303 (2009).
50. Miller, Y.I., Chang, M.K., Binder, C.J., Shaw, P.X. & Witztum, J.L. Oxidized low density lipoprotein and innate immune receptors. *Curr. Opin. Lipidol.* **14**, 437–445 (2003).
51. Miller, Y.I. *et al.* Minimally modified LDL binds to CD14, induces macrophage spreading via TLR4/MD-2, and inhibits phagocytosis of apoptotic cells. *J. Biol. Chem.* **278**, 1561–1568 (2003).
52. Dahinden, C.A. *et al.* Monocyte chemotactic protein 3 is a most effective basophil- and eosinophil-activating chemokine. *J. Exp. Med.* **179**, 751–756 (1994).
53. Bogunovic, M. *et al.* Identification of a radio-resistant and cycling dermal dendritic cell population in mice and men. *J. Exp. Med.* **203**, 2627–2638 (2006).
54. Niu, N., Laufer, T., Homer, R.J. & Cohn, L. Cutting edge: limiting MHC class II expression to dendritic cells alters the ability to develop Th2-dependent allergic airway inflammation. *J. Immunol.* **183**, 1523–1527 (2009).
55. Allenspach, E.J., Lemos, M.P., Porrett, P.M., Turka, L.A. & Laufer, T.M. Migratory and lymphoid-resident dendritic cells cooperate to efficiently prime naive CD4 T cells. *Immunity* **29**, 795–806 (2008).
56. Nakamura, Y. *et al.* Cigarette smoke extract induces thymic stromal lymphopoietin expression, leading to T_H2-type immune responses and airway inflammation. *J. Allergy Clin. Immunol.* **122**, 1208–1214 (2008).
57. Zhai, Y. *et al.* Cutting edge: TLR4 activation mediates liver ischemia/reperfusion inflammatory response via IFN regulatory factor 3-dependent MyD88-independent pathway. *J. Immunol.* **173**, 7115–7119 (2004).

ONLINE METHODS

Mice. C57BL/6 and BALB/c mice were from Charles River Laboratory. OT-II, DO11.10, CD11c-DTR, 4get, *Il4*$^{-/-}$, caspase-1-deficient and control NOD/ShiLtJ mice were from The Jackson laboratory. *Tlr2*$^{-/-}$, *Tlr3*$^{-/-}$, *Tlr4*$^{-/-}$, *Tlr6*$^{-/-}$, *Tlr7*$^{-/-}$, *Tlr9*$^{-/-}$, *Myd88*$^{-/-}$, *Ticam1*$^{lps-2/lps-2}$ mice were from S. Akira. *Nalp3*$^{-/-}$, *Ipaf*$^{-/-}$ and *Asc*$^{-/-}$ mice were provided by V. Dixit. Langerin-EGFP-DTR mice were from K.A. Hogquist. All animal protocols were reviewed and approved by the Institute Animal Care and Use Committee of Emory University.

Reagents. Endotoxin-free OVA was from Profos. CpG-B and Ultrapure LPS (*Escherichia coli* serotype 0111:B4) were from Invivogen. Papain, diphtheria toxin, NAC, tempol, pertussis toxin and BW245C were from Sigma Aldrich. The RNA Mini kit for RNA isolation and RT-PCR kit were from Qiagen. The SuperScript First-Strand Synthesis System for cDNA generation was from Invitrogen. Recombinant mouse IL-12 was from PeproTech. Papain and OVA were labeled with Alexa Fluor 488 carboxylic acid, 2,3,5,6-tetrafluorphenyl ester (A30005) and Alexa Fluor 647 carboxylic acid or succinimidyl ester (A20006) according to the manufacturer's instructions. Tempol-containing poly(ketal) microparticles were synthesized as described[45] with slight modifications.

Antibodies. Purified anti–mouse CD16-CD32 (2.4G2), anti-CD28 (37.51), anti-CD3ε (145-2c11), anti-CD11c (N418), anti-CD4 (GK1.5), anti-CD8 (53-6.7), anti-CD45 (30-F11), anti-CD45RA (14.8), anti-B220 (RA3-6B2), anti-IA-E (2G9), anti-CD49b (DX5), anti-CD62L (MEL-14), anti-IgE (23G3), antibody to T cell antigen receptor α-chain variable region 2 (B20.1) or β-chain variable region 5 (MR9-4), anti-IL-4 (11B11) and anti-IFN-γ (XMG1.2) were from BD Pharmingen. Anti–mouse Thy-1.2 (53-2.1) was from eBioscience. Purified anti–mouse CD3ε (145-2c11) was from Biolegend. Phycoerythrin-conjugated antibody to mouse TSLP receptor (FAB5451P) and neutralizing antibody to mouse TSLP (152614) were from R&D Systems. Anti–mouse CD205 (NLDC145) was from Serotec. Anti-mouse EO6 was provided by J. Witztum. Fluorescein-conjugated F(ab′)$_2$ goat anti–mouse IgM, μ-chain specific (115-096-020), was from Jackson Immunoresearch. Antibody to mouse TSLP (L-18) was from Santa Cruz Biotechnology. Alexa Fluor 488–conjugated donkey anti–goat IgG (A11055) was from Invitrogen.

Immunization. C567BL/6 mice were immunized subcutaneously at the base of tail with 100 μg OVA plus 50 μg adjuvant (papain, bromelain or CpG) in 100 μl PBS. In some experiments, mice were boosted on days 7 and 14. Serum was collected on day 14 after the first immunization, and titers of IgG1, IgG2b or IgE anti-OVA were analyzed by ELISA. On day 21 after primary immunization, draining lymph node cells were isolated and then restimulated for 4 d *in vitro* with OVA. In some experiments, mice were immunized subcutaneously with 50 μg papain or bromelain only. For blockade of ROS by NAC, 4get mice were subcutaneously injected at the base of tail once daily with NAC (150 mg per kg body weight) from 2 d before to 3 d after immunization. For blockade of ROS in DCs *in vivo*, 6 mg poly(ketal) microparticles containing 300 μg tempol were injected into 4get mice subcutaneously at the base of the tail 24 h before immunization with OVA plus papain. In some experiments, 4get mice were injected subcutaneously with 0.5 μg pertussis toxin or 100 nM (100 μl) BW245c daily for 4 d at the site of immunization for inhibition of cell migration. For adoptive transfer of OT-II T cells, CD11c$^-$CD11b$^-$CD4$^+$ splenic T cells were purified by removal of CD11c$^+$ and CD11b$^+$ cells with anti-CD11c and anti-CD11b microbeads and the negative fraction was enriched for CD4$^+$ T cells with anti-CD4 microbeads. For analysis of proliferation, CD4$^+$ T cells were labeled with CFSE (carboxyfluorescein diacetate succinimidyl ester; Invitrogen).

Stimulation of lymphocytes. Draining lymph node cells were isolated by digestion for 20 min at 37 °C with collagenase type 4 (Worthington Chemicals). Samples were enriched for CD11c$^+$ DCs by positive selection with anti-CD11c magnetic beads (Miltenyi Biotech). For isolation of DC subsets, enriched CD11c$^+$ cells were stained with fluorescein isothiocyanate–conjugated anti-CD205 (NLDC-145), phycoerythrin-conjugated anti-CD45RA, peridinin chlorophyll protein–cyanine 5.5–conjugated anti-CD8α and allophycocyanin-conjugated anti-CD11c. Cells were sorted on a FACSAria. For isolation of basophils, draining lymph nodes were isolated 3 d after immunization of mice with papain plus OVA, then samples were enriched for basophils with anti-CD49b microbeads and then labeled with anti-CD49b and anti-IgE. CD49b$^+$IgE$^+$ cells were sorted by flow cytometry with a purity of >90%. Naive isolation of CD4$^+$ T cells first involved enrichment with anti-CD4 microbeads, followed by sorting of CD4$^+$CD62L$^+$ cells by flow cytometry. For *ex vivo* coculture of DCs, basophils and T cells, sorted CD11c$^+$B220$^-$ (conventional) DCs (5×10^3 to 10×10^3) or basophils (5×10^3 to 10×10^3) were cultured for 3–5 d with naive CD4$^+$ T (1×10^5) cells in 96-well round-bottomed plates in the presence of IL-3 (10 ng/ml; R&D Systems). Proliferation was assessed by [^{3}H]thymidine incorporation through the addition of ^{3}H-labeled thymidine (Amersham Life Sciences) to cells during the final 16 h of culture. For *in vitro* stimulation, purified splenic or lymph node DCs (1×10^4) were cultured with naive CD4$^+$ T cells (1×10^5) and OVA peptide (amino acids 329–339 (ISQVHAAHAEINEAGR); 10 μg/ml) in 200 μl complete RPMI medium (10% (vol/vol) FBS (vol/vol Cellgro), 2 mM L-glutamine (Gibco Invitrogen), 0.01 M HEPES (Lonza), pH 7.2, 1 mM sodium pyruvate (Lonza), 200 U/ml of penicillin-streptomycin (Lonza) and 0.055 mM β-mercaptoethanol (Gibco Invitrogen)) in 96-well round-bottomed polystyrene plates. In some experiments, papain (25 μg/ml), NAC (1.5 mM), anti-IL-12 (1 μg/ml; C18.2; eBioscience) or anti-CD70 (3 μg/ml; RF70; eBioscience) was added to cultures.

Isolation of dermal cells. Excised ear tissues were separated for exposure of the dorsal and ventral sides of the skin sheets and were allowed to float for 1 h at 37 °C with the dermal side down in a 0.25% (wt/vol) trypsin solution containing 2.5 mM EDTA. Epithelial sheets were peeled carefully from the dermis with forceps. Dermal sheets were minced into small pieces and were digested for 1.5–2 h at 37 °C with collagenase 4 (1 mg/ml) in complete RPMI-1640 medium for isolation of dermis-specific cells.

Immunohistology. Mice were killed at the appropriate time points and skin patches were isolated and snap-frozen in optimum cutting temperature compound (Triangle Biomedical Sciences), followed by immunofluorescence staining of sections 8–10 μm in thickness. For TSLP staining, air-dried sections were fixed with acetone for 10 min at −20 °C, followed by blocking for 30 min with antibody 2.4G2. Sections were blocked for 30 min at 25 °C with buffer containing 1% (wt/vol) BSA, 10% (vol/vol) donkey serum and 1% (wt/vol) 2.4G2, and were incubated for 2 h at 25 °C with goat anti–mouse TSLP (1:500 dilution; L-18; sc-19177; Santa Cruz Biotechnology). After samples were washed with PBS, Alexa Fluor 488–conjugated donkey anti–goat IgG (A11055; Invitrogen) was added for 1 h at 25 °C. For staining with EO6, sections were blocked with 10% (vol/vol) goat serum and were stained with EO6 (1 μg/ml). Fluorescein isothiocyanate–conjugated goat anti–mouse IgM (115-096-020; Jackson Immunoresearch was used as secondary antibody. All slides were mounted in Prolong antifade medium (Molecular Probes). Images were obtained with a Zeiss LCM510 confocal microscope. For staining of Langerhans cells, epidermal sheets were prepared and fixed in acetone for 10 min at −20 °C, followed by blocking for 30 min at 25 °C with 2.4G2 and incubation overnight at 4 °C with fluorescein isothiocyanate–conjugated anti–mouse IA-E.

Staining of ROS. For *in vitro* staining in DCs, total CD11c$^+$ lymph node DCs were stimulated *in vitro* overnight at 37 °C with papain (25 μg/ml). ROS were stained with the Image-iT LIVE Green Reactive Oxygen Species Detection kit according to the manufacturer's instructions (Invitrogen). For studies *in vivo*, C57BL/6 mice were injected subcutaneously with 50 μg papain, then cells from the draining lymph nodes were isolated 2 h later and incubated for 30 min at 37 °C with a solution of 25 μM DCF (5-(and-6)-carboxy-2′,7′-dichlorodihydrofluorescein diacetate) in PBS. After being washed twice with PBS, cells were labeled with anti-CD11c and anti-CD45R (B220). For the identification of ROS in skin sections *in vivo*, mice were injected subcutaneously with 20 μg hydro-Cy5 at the site of immunization 1 h before tissue was collected. Skin patches were snap-frozen in optimum cutting temperature compound, then were cut into cryosections and labeled with Alexa Fluor 488–conjugated anti-CD11c. Images were captured by with a Zeiss LCM510 confocal microscope as described above.

Depletion of lineage-specific cells *in vivo*. For depletion of CD11c$^+$ cells *in vivo*, CD11c-DTR mice or littermate control mice received an intraperitoneal injection of diphtheria toxin (100 ng per mouse) 1 d before immunization[27]. For

doi:10.1038/ni.1883

depletion of Langerhans cells, langerin-DTR mice received an intraperitoneal injection of diphtheria toxin (1 μg per mouse) 14 d before immunization. Ablation efficiency was monitored by analysis of DCs in lymph nodes, dermis or epidermal sheets. For depletion of basophils *in vivo*, mice were injected twice daily for 3 d with 5 μg anti-FcεRIα (MAR-1)[10]. The efficiency of basophil depletion was analyzed in peripheral blood 24 h after injection on day 3. For T cell depletion, mice were given daily intravenous injection of 40 μg anti-CD3 from 5 d before to 2 d after immunization.

ELISA. Titers of IgG1, IgG2a, IgG2b anti-OVA were assessed by ELISA as described[26]. IgE ELISA was done as described[58]. Cytokines in culture supernatants were detected with the OptEIA Set for sandwich ELISA from BD Biosciences.

Intracellular cytokine staining and analysis. $CD4^+$ T cells in culture for 4–5 d were restimulated for 5 h with anti-CD3 (10 μg/ml) and anti-CD28 (2 μg/ml) in 96-well flat plates (Nunc) in the presence of GolgiStop (BD Pharmingen). Cells were stained with fluorescein isothiocyanate–conjugated anti-CD4, were made permeable with Cytofix/Cytoperm (BD Biosciences) and were stained with phycoerythrin-conjugated anti-IL-4 (11B11; BD) and allophycocyanin-conjugated anti-IFN-γ before analysis on a FACSCalibur.

Microarray analysis. Total RNA was extracted from lymph node DCs stimulated *in vitro* with papain (25 μg/ml) or LPS (1 μg/ml) with an RNeasy kit (Qiagen). RNA quality was assessed with an Agilent Bioanalyser 2100, and only RNA with minimal degradation and distinct 18*S* and 28*S* rRNA bands was used for analysis. The Vanderbilt Microarray Facility did microarray processing. Fragmented and biotin-labeled cDNA was synthesized from 100 ng purified mRNA with the Ovation Biotin system (Nugen). The cDNA was hybridized to GeneChip MouseGenome 430 2.0 Array chips (Affymetrix). Hybridized chips were stained and washed and were scanned with a GeneArray scanner (Affymetrix). GeneSpring software (Silicon Genetics) was used for data analysis.

Statistics. The statistical significance of differences between groups was calculated with a two-tailed Student's *t*-test or one-way analysis of variance. *P* values of less than 0.05 were considered statistically significant.

58. McGowen, A.L., Hale, L.P., Shelburne, C.P., Abraham, S.N. & Staats, H.F. The mast cell activator compound 48/80 is safe and effective when used as an adjuvant for intradermal immunization with *Bacillus anthracis* protective antigen. *Vaccine* **27**, 3544–3552 (2009).